nature neuroscience

Learning to expect the unexpected: rapid updating in primate cerebellum during voluntary self-motion

Jessica X Brooks[1,2], Jerome Carriot[1,2] & Kathleen E Cullen[1]

There is considerable evidence that the cerebellum has a vital role in motor learning by constructing an estimate of the sensory consequences of movement. Theory suggests that this estimate is compared with the actual feedback to compute the sensory prediction error. However, direct proof for the existence of this comparison is lacking. We carried out a trial-by-trial analysis of cerebellar neurons during the execution and adaptation of voluntary head movements and found that neuronal sensitivities dynamically tracked the comparison of predictive and feedback signals. When the relationship between the motor command and resultant movement was altered, neurons robustly responded to sensory input as if the movement was externally generated. Neuronal sensitivities then declined with the same time course as the concurrent behavioral learning. These findings demonstrate the output of an elegant computation in which rapid updating of an internal model enables the motor system to learn to expect unexpected sensory inputs.

How does the brain allow us to acquire new skills and maintain mastered skills in response to changes in the external environment and our motor systems? There are many reasons to believe that it does this by computing a sensory prediction error signal that represents the difference between the expected and actual sensory consequences of a given motor command. First, the intrinsic delays of sensory feedback make it impossible for sensory signals alone to account for many aspects of motor learning[1–5]. Second, theoretical investigations have demonstrated that the computation of sensory prediction errors is essential for fine-tuning motor behavior, including its on-line control and motor adaptation[6,7]. Third, behavioral studies in humans suggest that errors induced by external perturbations are interpreted as sensory prediction errors[8,9].

The cerebellum, a structure that is well-conserved across vertebrates, has a vital role in motor learning. Numerous studies have focused on understanding the information represented by the activity of cerebellar Purkinje cells, whose axons encode the output of the cerebellar cortex, during motor learning (reviewed in refs. 10,11). Although progress has been limited by the inherent challenge of systematically dissociating motor commands and movement kinematics, recent experiments have shown that Purkinje cells encode signals consistent with a forward model (that is, the predicted sensory consequence of movement) rather than actual movement[12,13]. Theoretically, sensory prediction errors will occur if there is a mismatch between the sensory expectation computed by the cerebellum's forward model and actual sensory feedback (**Fig. 1a**). This error signal has been hypothesized to fine-tune the cerebellum's forward model, as well as the consequent motor command, to ensure accurate motor learning (reviewed in refs. 14,15). Although the finding that cerebellar patients exhibit deficits in the predictive control of movement[16–18] is consistent with this proposal, the existence of an explicit neural representation of such an error signal has not yet been demonstrated.

Thus, to date, the question of where and how the brain compares expected and actual sensory feedback during the process of motor learning remains open. One recent line of work reported that Purkinje cells encode both predictive signals and actual sensory feedback during manual tracking[13,19]. However, this work stopped short of linking neuronal activities to sensory prediction errors, as the predictive and feedback representations in individual Purkinje cells were separated by several hundred milliseconds. Accordingly, we examined whether there might be evidence for the comparison between predictive and feedback signals required for the computation of sensory prediction errors downstream of Purkinje cells at the level of the deep cerebellar nuclei.

We took advantage of a relatively simple sensory-motor pathway with a well-described organization to gain new insight into the computations performed by the cerebellum to drive motor learning as well as its extinction. The most medial of the deep cerebellar nuclei (rostral fastigial nucleus, rFN) constitutes a major output target of the cerebellar cortex[20], and this nucleus in turn sends strong projections to the vestibular nuclei (VN), reticular formation and spinal cord[20–23] for postural control. While monkeys made voluntary head movements, we unexpectedly applied a load to the head and recorded from single neurons in this deep cerebellar nucleus. We found that neurons displayed responses consistent with the initial introduction of a sensory prediction error as well as its subsequent decline throughout motor learning. We further observed corresponding parallel changes in the responses of neurons downstream in the VN, thereby directly linking observed changes in cerebellar output to sensory-motor adaptation during voluntary head motion.

RESULTS

To study the neural basis of motor learning during voluntary head movements, we recorded from single neurons (n = 41) in the rFN

[1]Aerospace Medical Research Unit, Department of Physiology, McGill University, Montreal, Canada. [2]These authors contributed equally to this work. Correspondence should be addressed to K.E.C. (kathleen.cullen@mcgill.ca).

Received 17 February; accepted 3 July; published online 3 August 2015; doi:10.1038/nn.4077

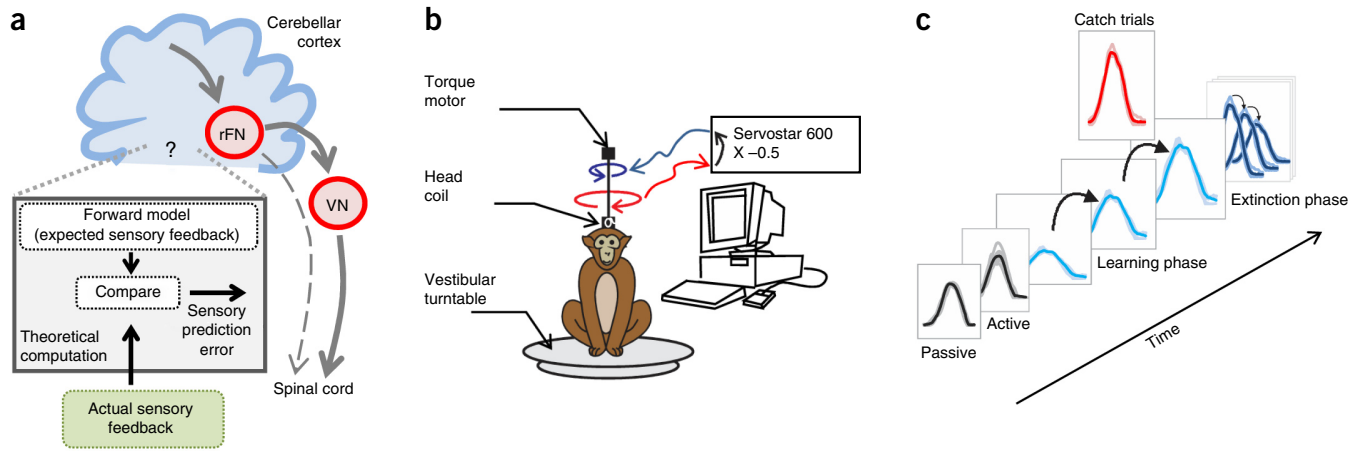

Figure 1 Experimental design. (**a**) Schematic showing the prevailing model of the proposed circuit for motor learning in which the cerebellum computes an estimate of the expected sensory consequence of the brain's motor command (that is, forward model). This estimate is then compared with the actual sensory feedback to compute the sensory prediction error. Single-unit recordings were made in the rFN, which constitutes a major output target of the cerebellar cortex, as well as VN, which project to the spinal cord. (**b**) Experimental set-up for learning procedure in which resistive torque was applied to reduce head motion initially by half. (**c**) Sequence of learning task. First, head movements and neuronal responses (not shown) were recorded before learning in both passive and active conditions. Second, the load was applied and held constant for the learning phase. Third, after the learning phase, the motor was randomly turned off for single catch trials. Finally, the motor was completely turned off for the extinction phase.

and quantified their sensitivity to passively applied stimulation of the vestibular system and neck proprioceptors[24]. Because we focused on head movement motor learning, we targeted our analyses on the responses of unimodal rFN neurons (hereafter referred to simply as rFN neurons, $n = 21$), as these neurons respond to head motion. Bimodal rFN neurons instead responded to body motion, consistent with previous results[24] (**Supplementary Figs. 1–5**). Recordings were also made from neurons in the VN that responded to passive vestibular stimulation, but were insensitive to eye movements as well as passive neck stimulation, consistent with previous characterizations of VN vestibular-only neurons[25].

Deep cerebellar nuclei during learning: evidence for computation of sensory prediction error

In a typical learning experiment, the monkey first made active head movements between two targets located 50 degrees apart. Then, after at least 20 of these control movements, we introduced a load to the head by applying resistive torque (**Fig. 1b**) proportional to head velocity adjusted to produce an initial reduction in peak head velocity of about 50%. The monkey then made >60 learning trials under the new biomechanical constraints imposed by this new load (that is, learning phase; **Fig. 1c**). After 50 learning trials, occasional 'catch trials' (**Fig. 1c**) were introduced to assess neuronal responses when the load was unexpectedly removed for a single trial. Finally, the load was permanently removed and the monkey continued to make orienting movements during the learning extinction phase (**Fig. 1c**).

In conditions that do not involve motor learning, rFN neurons encode passively generated, but not self-produced (that is, active), vestibular sensory signals[26]. The responses of a typical neuron before learning are shown in **Figure 2a**. Consistent with previous work[26], the marked difference in the modulation of this representative neuron during passive (0.43 ± 0.04 spikes per s/° per s) and active (0.05 ± 0.04 spikes per s/° per s) head motion was typical of our population (**Fig. 2a**). Overall, the sensitivity of rFN neurons was significantly reduced (~70%) during active motion (0.10 ± 0.01 versus 0.35 ± 0.03 spikes per s/° per s; Wilcoxon test, $P = 4.2517 \times 10^{-7}$). Thus, these neurons preferentially responded to exafferent (externally generated) as compared with reafferent (self-generated) sensory effects of self-motion, consistent with the coding of unexpected sensory input. If rFN neuronal responses are updated in a manner consistent with the computation of sensory prediction error signals, we hypothesized that they should robustly encode reafferent sensory input when the relationship between motor commands and resulting head motion is altered, but their sensitivity should then decrease with learning. Specifically, neurons should show an increased sensitivity to head motion when the load is initially applied and show markedly decreased head-velocity sensitivity once adaptation occurs, consistent with the brain's updating of the predicted sensory consequence of movement.

To test these hypotheses, we analyzed changes in the trial-by-trial motor behavior and neuronal responses during the learning phase of our procedure (**Fig. 2a**). Peak head velocity was initially reduced by approximately 50% (64 ± 4 versus 173 ± 12° per s) and then progressively increased, reaching values that were not significantly different from those of control movements (161 ± 8° per s for the 46st to 50th movements versus 173 ± 12° per s, respectively; Wilcoxon test, $P = 0.082$). Thus, the monkey successfully modified its head motor command to account for the new relationship between motor command and movement. Notably, when the torque was initially applied, an example rFN neuron robustly responded to active motion (**Fig. 2a**). Indeed, the neuron's sensitivity to vestibular stimulation resulting from passive head motion provided an excellent prediction of its response to active head motion during the early phases of learning, but this prediction increasingly overestimated the neuron's response for head movements made in the middle and later phases of learning (**Fig. 2a**). Notably, the neuron's head-velocity sensitivity progressively decreased such that it was nearly negligible once the monkey had adapted to the new load, by about trial 50; as the magnitude of the difference between expected and actual sensory input (that is, head velocity error) approached zero, neuronal sensitivity progressively decreased (**Fig. 2b**,**c**). Thus, consistent with our prediction, the example rFN neuron responded robustly to reafferent sensory input when the relationship between motor command and movement was initially altered, followed by a markedly decreased modulation once motor adaptation had occurred.

To establish that the brain's internal model had been updated to account for the imposed perturbation, we next introduced catch

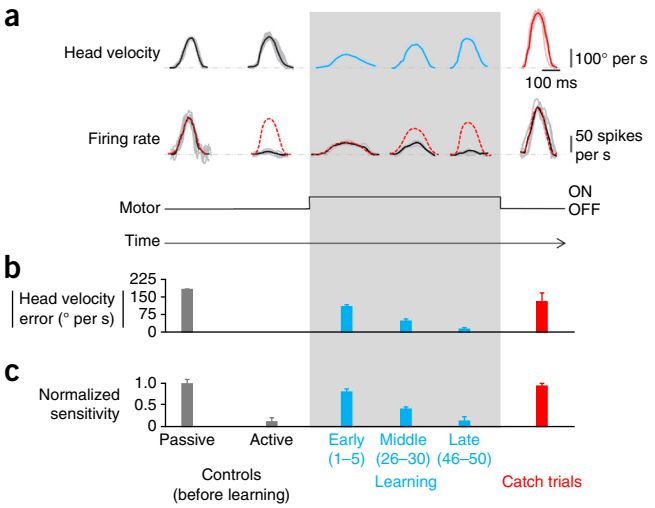

Figure 2 Learning procedure. (**a**) Activity of an rFN example neuron during the learning phase and catch trials. The top row shows the head velocity during control trials, learning phase and catch trials overlaying five trials. The second row shows the firing rates corresponding to the head movements above. Gray lines show individual trials and black lines show the average. The red dashed lines superimposed on the firing rates are a prediction based on the neuron's sensitivity to passive whole-body rotation. (**b**) Head velocity error magnitude during learning and catch trials ($n = 5$ for each condition). When the load was applied, the monkey initially made slower head movements, as quantified by a significant head velocity error. As learning progressed, head velocity increased, nearing control values, as indicated by the marked decrease in head velocity error magnitude (light blue bars). (**c**) Normalized sensitivity to the corresponding head movements ($n = 5$ for each condition) shown above. During the learning phase, the neuronal sensitivity gradually decreased from that measured during passive head motion to the suppressed response observed during active motion (light blue bar). Neuronal sensitivity during catch trials (red) was comparable to the neuronal sensitivity during early learning and passive head movements. Error bars represent ±s.e.m.

trials[27–30] by unexpectedly removing the applied load. Indeed, because the head motor system had incorporated the applied resistive load into its motor plan, monkeys made substantially faster head movements when the load was unexpectedly removed (281 ± 11° per s; **Fig. 2a**). Moreover, neurons again showed robust responses to reafferent sensory input when the load was removed. Indeed, the example neuron was typical in that its response to vestibular stimulation resulting from passive head motion again provided an excellent prediction of its response to active head motion during catch trials (**Fig. 2a**), indicating the vestibular sensitivity was comparable to that observed for passive rotations (Wilcoxon test, $P > 0.05$; **Fig. 2b**). Thus, following the introduction of a large sensory prediction error by either application of the load to induce learning or removal of the load during catch trials, neurons initially responded with the same sensitivity as during passive motion, regardless of the error's sign (that is, less versus more head velocity than expected, respectively). For completeness, a comparable analysis was also carried out on bimodal neurons (**Supplementary Fig. 1**), confirming the expected lack of response before, during and after learning, as these neurons respond to body rather than head motion[24].

The observations shown in **Figure 2** were representative and are summarized in **Figure 3a**,**b** for our population. Consistent with our experimental design, passively applied head velocities were comparable to active head movements made before the induction of learning (165 ± 10 versus 180 ± 20° per s, respectively; Wilcoxon test, $P = 0.0937$; **Fig. 3a**). Moreover, similar to the behavior recorded simultaneously from the example neuron (**Fig. 2**), the peak head velocity of active head movements dropped by ~50% when the load was first applied to the head, steadily increased returning to control values after ~50 movements and nearly doubled for catch trials (**Fig. 3a**). Notably, these changes in head movement were consistently linked to changes in neuronal responses across our population of neurons (**Fig. 3b**). Neuronal responses to active movements were minimal before learning, but were robust immediately after the onset of learning and were in fact characterized by sensitivities comparable to those estimated for passive motion (0.28 ± 0.04 versus 0.35 ± 0.03 spikes per s/° per s; Wilcoxon test, $P = 0.3327$). As learning progressed, neurons displayed increasingly reduced vestibular sensitivities that returned to control values for active motion within 50 trials (0.09 ± 0.01 spikes per s/° per s; Wilcoxon test, $P = 0.9599$). In addition, comparison of neuronal responses during catch trials revealed sensitivities comparable to those measured during passively applied motion (0.33 ± 0.05 spikes per s/° per s; Wilcoxon test, $P = 0.8307$; **Fig. 3b**). As expected, a comparable analysis of our population of bimodal rFN neurons, which encode body rather than head motion, did not show any changes in response sensitivity during head movement learning (**Supplementary Fig. 2**). Thus, taken together, these results suggest a tight linkage between the learning of new relationships between motor commands and actual head movements and changes in the response sensitivity of neurons in the deep cerebellum that is consistent with the coding of unexpected sensory input.

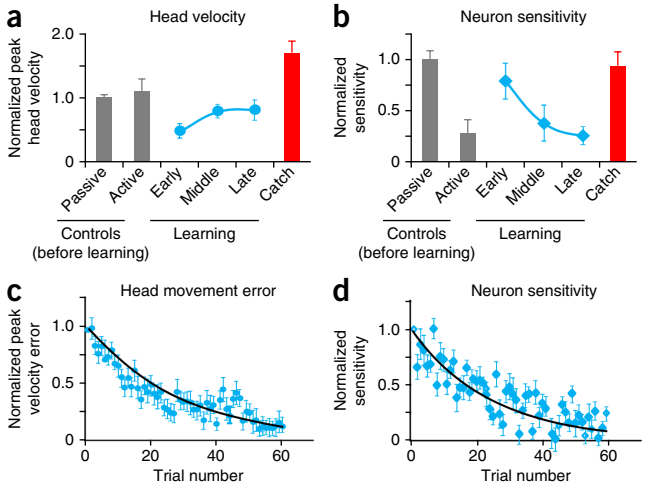

Figure 3 Average head velocity and sensitivity for our population of rFN neurons ($n = 21$) during the learning phase. (**a**) Normalized head velocity for control trials before learning, learning phase and catch trials. (**b**) Normalized neuronal sensitivity for control trials, the learning phase and catch trials. Data show average and error bars represent ±s.e.m. in all panels. (**c**) Scatter plot of peak head velocity errors over time for each trial during the learning phase. (**d**) Scatter plot of normalized neuronal sensitivity over time for each trial during the learning phase. Black lines show exponential fits to the data.

Dynamics of the time course of adaptation

Previous studies of motor learning have shown that adaptation can occur within ten repetitions of a task (for example, compensation for coriolis forces when reaching in a rotating environment[28,31]) or require much more prolonged exposure (for example, reaching while forces dependent on the motion state of the hand are applied[32]). To determine the time course of behavioral learning and corresponding changes in neuronal activity in our motor learning task, we next performed a trial-by-trial

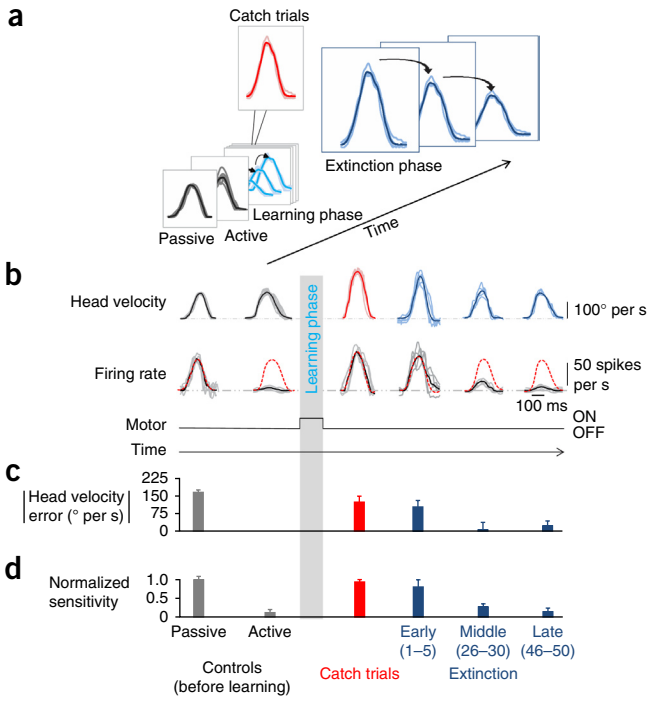

Figure 4 Extinction phase. (**a**) Last phase of the procedure, during which the torque motor was turned off (extinction phase). (**b**) Activity of the example neuron shown in **Figure 2** during the extinction phase. The top row shows the head velocity during the extinction phase overlaying five trials. The second row shows the firing rates corresponding to the head movements shown above. Gray lines show individual trials and black lines show the average. The dashed red lines superimposed on the firing rates are a prediction based on the sensitivity estimated during passively applied whole body rotation. (**c**) Head velocity error magnitude during learning extinction ($n = 5$ for each condition). When the load was removed, the monkey initially made faster head movements, and head velocity error then progressively decreased as head velocity approached control values (dark blue bars). (**d**) Normalized neuronal sensitivity for the extinction phase ($n = 5$ for each condition). Data show average and error bars represent ±s.e.m. in **c** and **d**. Data from the control (before learning) and catch trials are reproduced here for comparison.

analysis of each single neuron's response (**Supplementary Fig. 3a**,**b**). We quantified the time course of the change in peak head velocity and compared it to that of the accompanying decrease in neuronal sensitivity by fitting both data sets with exponential curves (Online Methods). We examined the average normalized change in velocity (Online Methods and **Fig. 3c**) and normalized neuronal sensitivities for each trial in the learning phase (**Fig. 3d**) across our population of rFN neurons. Over our population, the average time constant of the increase in peak velocity toward control values was markedly similar to the average time constant for the coincident decrease in neuronal sensitivity (34 ± 7 versus 24 ± 8 trials, respectively; Wilcoxon test, $P = 0.3944$). Thus, our results demonstrate that the decreased neuronal sensitivity of deep cerebellar nuclei neurons tracks the detailed time course of behavioral changes as learning progresses.

Neuronal responses during extinction

We next addressed whether rFN neuronal responses are also updated in a manner consistent with the computation of sensory prediction error signals when the relationship between motor command and movement was altered after learning had occurred and the load was permanently removed (that is, during the extinction phase of learning; **Fig. 4a**). We found that head movements were initially (that is, the first five movements made in the extinction phase) larger than control head movements (274 ± 11° per s versus 173 ± 12° per s, Wilcoxon test, $P = 9.9632 \times 10^{-13}$) as would be expected since these trials were effectively equivalent to catch trials (catch trials; **Fig. 4b**). When the monkey then continued to make active movements without the load, peak head velocity returned to normal (extinction; **Fig. 4b**). Furthermore, we found that rFN neuron responses mirrored the extinction of this learned behavior. **Figure 4b** illustrates the responses of the same example neuron shown in **Figure 2** during learning extinction (**Fig. 4b**–**d**). In the early phases of extinction, the example neuron's response gain was comparable to its sensitivity to passive stimulation (0.34 ± 0.08 versus 0.43 ± 0.04 spikes per s/° per s, respectively; **Fig. 4d**). In contrast, in the late stages of extinction, its response gain was substantially reduced and comparable to its sensitivity to active rotations made before learning (0.05 ± 0.05 versus 0.05 ± 0.04 spikes per s/° per s, respectively; **Fig. 4d**). Thus, these findings are consistent with the idea that rFN neuronal sensitivity dynamically tracks the comparison of expected and actual head movement; response gain was initially comparable to that observed for passive motion and then rapidly decreased to levels observed during actively generated head movements in a manner that closely paralleled the reduction in head velocity error (**Fig. 4c**,**d**).

The observations shown in **Figure 4** were representative and are summarized in **Figure 5a**,**b** for our population. When the torque was initially removed, peak head velocity increased (early extinction), but then steadily decreased until it reached near control values (late extinction; **Fig. 5a**). As expected, the peak head velocities observed during the first few movements after the torque had been removed (that is, early extinction) and catch trials were not significantly different (274 ± 19° per s versus 281 ± 18° per s; Wilcoxon test, $P = 0.1464$). Notably, changes in neuronal sensitivity mirrored these behavioral changes. Initially, the vestibular sensitivities of rFN neurons were comparable to those measured in response to passively applied motion (0.35 ± 0.04 spikes per s/° per s, early extinction; Wilcoxon test, $P = 0.8111$; **Fig. 5b**). Then, once the learned behavior was extinguished (that is, the peak velocity of head movement returned to control values), response sensitivities were markedly reduced and, in fact, comparable to those measured for active movements in the control condition (0.05 ± 0.01 spikes per s/° per s, late extinction; Wilcoxon test, $P = 0.0509$; **Fig. 5b**).

The extinction of learning is typically faster than the initial learning (reviewed in ref. 33). We quantified the time course of extinction and the corresponding changes in rFN neuronal activity to see whether this was the case for head-control motor learning. We again performed a trial-by-trial analysis of each single neuron's response and compared it to the time course of the change in peak head velocity (**Supplementary Fig. 3c**,**d**). **Figure 5c**,**d** illustrates the average normalized change in velocity (Online Methods) and normalized neuronal sensitivities for each trial in the extinction phase across our population of rFN neurons. To facilitate comparison with the time course of learning (**Fig. 3c**,**d**), we fit both data sets with exponential curves (Online Methods). Over our population of rFN neurons, the average time constant of the decrease in peak velocity toward control values was comparable to the average time constant for the coincident decrease in neuronal sensitivity (21 ± 8 versus 16 ± 7 trials, respectively; Wilcoxon test, $P = 0.9861$). Furthermore, comparisons with the time course of behavioral and neuronal changes in the learning phase revealed that both were indeed significantly shorter (~30%) for extinction (paired Wilcoxon tests; behavior, $P = 0.004$; neuronal, $P = 0.0421$). For completeness, comparable testing and analyses were

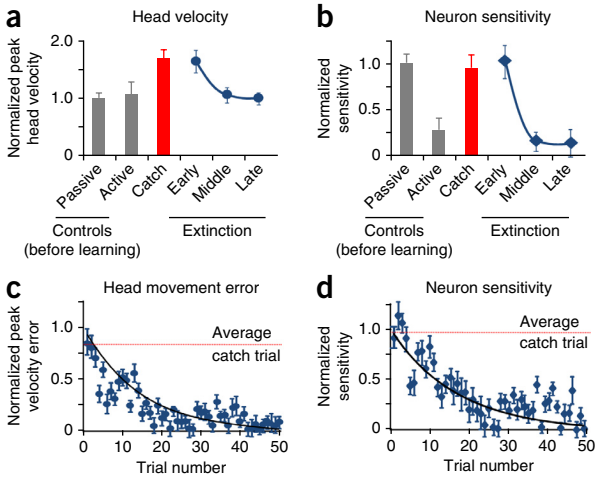

Figure 5 Average head velocity and sensitivity for our population of rFN neurons ($n = 21$) during the extinction phase. (**a**) Normalized head velocity for control trials before learning, catch trials and extinction phase. (**b**) Normalized neuronal sensitivity for control trials before learning, catch trials and extinction phase. Data show average and error bars represent ±s.e.m. in all panels. (**c**) Scatter plot of peak head velocity error over time for each trial during the extinction phase. (**d**) Scatter plot of normalized neuronal sensitivity over time for each trial during the extinction phase. Black lines show exponential fits to the data. Dashed lines are the average values for the catch trials.

carried out on bimodal neurons (**Supplementary Figs. 4** and **5**) that confirmed the expected lack of response throughout the entire time course of extinction. In summary, our trial-by-trial analysis revealed that the time course of the extinction of learning is linked to changes in the responses of rFN neurons in the deep cerebellar nuclei, providing evidence that the output of the cerebellum signals the mismatch between the expected and actual sensory consequences of head movement during the extinction as well as acquisition of learning.

Vestibular nuclei neurons mirror rFN neurons during motor learning

The deep cerebellar nuclei neurons of the rFN serve a vital role in regulating vestibulo-spinal reflexes to ensure accurate postural control. Given that the VN receive direct input from the rFN[20–23], we hypothesized that the modulation of VN neurons that mediate vestibulo-spinal pathways would similarly reflect the updating of the forward model predicting the sensory consequences of head motion, thereby encoding a continuously updated representation of unexpected motion that could be used to maintain postural stability. To directly test this hypothesis, we examined whether the time course of changes in the head-velocity sensitivity of VN neurons was linked on a trial-by-trial basis to the learning and extinction of new relationships between active motion and vestibular reafference. Before learning, VN neurons showed robust modulation for passive motion; however, their sensitivities were greatly reduced when motion was self-generated ($N = 20$, 0.46 ± 0.01 versus 0.13 ± 0.03 spikes per s/° per s), as has been previously reported[25,34].

Figure 6 illustrates the responses of a typical VN neuron before learning, during learning and catch trials, and during the extinction of learning. Consistent with our hypothesis, the trial-by-trial modulation of VN neurons similarly represented the updating of the internal model predicting the sensory consequences of head motion. **Figure 7** illustrates the comparison of the population response during the learning and extinction phases of learning. Neuronal sensitivities increased following the application of the load and then decreased during learning. Specifically, in the early stages of learning, sensitivities to vestibular stimulation produced by active motion were comparable to those produced by passive motion (0.46 ± 0.05 versus 0.46 ± 0.01 spikes per s/° per s; Wilcoxon test, $P = 0.8181$) and, by the late phase of learning, sensitivities to active motion were again suppressed to control levels (0.13 ± 0.04 spikes per s/° per s; Wilcoxon test, $P = 0.9461$). During catch trials, vestibular sensitivities were again comparable to those measured during passively applied motion (0.48 ± 0.06 spikes per s/° per s; Wilcoxon test, $P = 0.8392$). Notably, as seen for rFN neurons, VN neuronal sensitivity progressively decreased as the magnitude of the difference between expected and actual sensory input (that is, head velocity error) approached zero (**Fig. 7b,c**). Moreover, neuronal responses decayed with a time constant equivalent to that observed for rFN neurons (32 ± 7 versus 24 ± 8 trials; Wilcoxon test, $P = 0.3944$). Thus, neurons in the VN, like those in the deep cerebellar nuclei, demonstrate rapid updating as the motor system learns to expect unexpected vestibular input.

In addition, there was a marked and immediate increase in neuronal sensitivity at the onset of the learning extinction. Neuronal sensitivities then decreased to control levels with the same time course

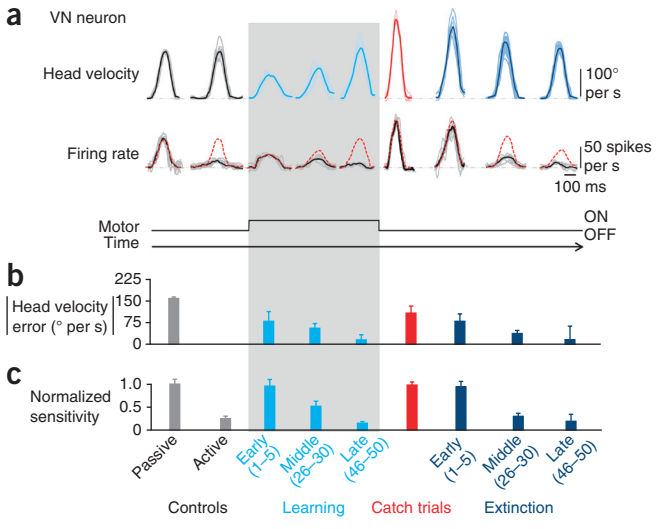

Figure 6 Activity of an example neuron recorded in the VN. (**a**) The top row shows the head velocity during control trials, learning phase, catch trials and extinction phase overlaying five trials. The bottom row shows the firing rates corresponding to the head movements above. Gray lines show individual trials and black lines show the average. The red dashed lines superimposed on the firing rates are a prediction based on the sensitivity estimated during passive whole-body rotation. (**b**) The magnitude of head velocity error during control, learning, catch and extinction trials ($n = 5$ for each condition). During the learning phase, the magnitude of head velocity error decreased (as head velocity increased) to approach control values (light blue bars). During the extinction phase (dark blue bars), the magnitude of head velocity error again decreased (this time as head velocity decreased) to approach control values (dark blue bars). (**c**) Normalized sensitivity to corresponding head movements shown above ($n = 5$ for each condition). During the learning phase, neuronal sensitivity gradually decreased from that observed during passive motion to the suppression seen for active motion (light blue bars). Neuronal sensitivity during catch trials (red) is comparable to the neuronal sensitivity during early learning and passive head movements. During the extinction phase, neuronal response sensitivity again gradually decreased from that observed during passive motion to the suppression observed for active motion (dark blue bars). Error bars represent ±s.e.m.

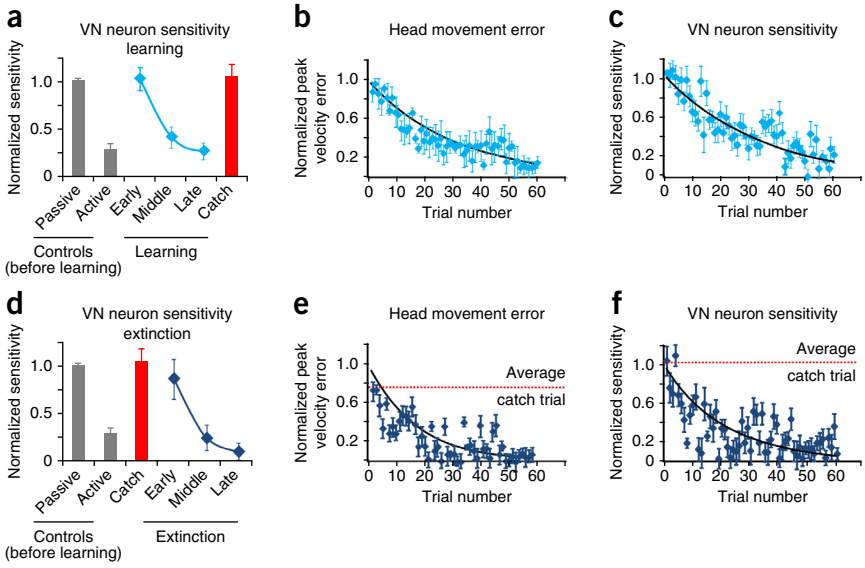

Figure 7 Average head velocity and neuronal sensitivity for our population of neurons recorded in the VN ($n = 20$). (**a**) Normalized neuronal sensitivity for control trials before learning and during learning phase and catch trials. (**b**) Scatter plots of head velocity error magnitude for each trial during learning. (**c**) Scatter plot of normalized neuronal sensitivity over time for each trial during learning phase. (**d**) Normalized neuronal sensitivity for control trials before learning, catch trials and extinction phase. (**e**) Scatter plots of head velocity error magnitude for each trial during learning the extinction of learning. (**f**) Scatter plot of normalized neuronal sensitivity over time for each trial during the extinction phase. The dashed lines denote the average value for the catch trials (**e**,**f**). Data show average and error bars represent ±s.e.m. in all panels.

as the extinction of the learned behavior (**Fig. 7d**). Initially, neuronal sensitivities to active movements were comparable to those measured for passive motion (0.39 ± 0.09 spikes per s/° per s; Wilcoxon test, $P = 0.3234$), but, by the late phase of extinction, vestibular sensitivities were suppressed to control levels (0.05 ± 0.02 spikes per s/° per s; Wilcoxon test, $P = 0.1670$). Our trial-by-trial–based analysis (**Supplementary Fig. 6**) further established that neuronal sensitivities progressively decreased during extinction as the magnitude of the difference between expected and actual sensory input (that is, head velocity error) approached zero (**Fig. 7e**,**f**). The time constant of this decrease was equivalent to that observed above for rFN neurons during the extinction of learning (VN, 16 ± 7; rFN, 13 ± 8). Thus, in the extinction phase, following the introduction of a large sensory prediction error by removal of the load, neurons again initially responded with the same sensitivity as during passive motion. Moreover, as was the case for rFN neurons, VN neuronal sensitivities increased to robustly encode sensory reafference when a sensory prediction error was introduced regardless of direction of the error (that is, during learning initiation as well as during catch trials and extinction initiation). Taken together, our findings indicate that the sensory responses of individual neurons in the VN, similar to those in the deep cerebellar nuclei, reflect the dynamic computation of sensory prediction error as motor learning (and unlearning) progresses.

DISCUSSION

Our central finding is that rapid updating in the primate cerebellum, consistent with the dynamic comparison between expected and actual sensory feedback, enabled the motor system to learn to expect unexpected sensory input. Specifically, our results provide direct evidence that the sensitivity of individual cerebellar output neurons tracks the difference between predictive and feedback signals, consistent with the computation of sensory prediction error during motor learning. This conclusion is based on the trial-to-trial evaluation of neuronal responses and behavior before, during and after learning.

By applying a constant load while monkeys generated voluntary head movements, we were able to systematically alter the relationship between the motor command to move the head and its actual motion. Notably, analysis of trial-by-trial changes in neuronal responses revealed the rapid, but gradual (that is, not a switch-like transition), updating of an internal model, consistent with the resultant behavioral learning. Furthermore, as predicted, neurons again immediately showed increased vestibular sensitivity with the introduction of a new challenging sensory prediction error when the load was removed in catch trials, and neuronal response gain during learning extinction declined with the same time course as that of the behavior. To the best of our knowledge, these findings reveal for the first time the output of an elegant computation by which the cerebellum compares expected and unexpected sensory inputs to fine-tune behavior during motor learning.

Evidence for the updating of a forward model predicting the sensory consequences of voluntary motion

The computation of sensory prediction errors has emerged as an important theoretical concept in motor control (reviewed in refs. 14,15). In this context, the cerebellum has been proposed as a likely candidate site for a forward model that predicts the expected sensory consequences of self-generated action. Changes in motor apparatus and/or environment will cause a mismatch between the cerebellum's prediction and the actual resulting sensory stimulation. This mismatch is the sensory prediction error, which is thought to update both the forward model and motor program during motor learning to ensure that sensory-motor pathways remain calibrated. A major contribution of our study is that our results provide answers to the fundamental question of whether the brain actually compares predictive and feedback sensory signals during motor learning, and, if so, whether there is evidence for this computation at the level of the output neurons of the cerebellum.

Behavioral and lesion studies have provided clear evidence that the cerebellum has a fundamental role in motor learning. Notably, patients with cerebellar pathologies display impaired performance during sensory-motor adaptation tasks, characterized by persistent error and attenuated after-effects[18,35–37]. Targeted lesions of the cerebellum in primates similarly impair adaptation of voluntary eye movements and the vestibulo-ocular reflex[38,39]. Motor adaptation studies in humans have further suggested that learning requires updating of forward models, and that the errors produced by external perturbations are interpreted as sensory prediction errors rather than target errors[8,9]. Indeed, when high-quality sensory feedback is available, adaptation of motor commands appears to be almost exclusively driven by sensory prediction errors[40]. The cerebellum is required for this computation, as patients show selective deficits in sensory-motor learning, consistent with a cerebellar-dependent adaptation process based on minimizing such errors[17].

By assessing trial-by-trial changes in firing rate, we found that the sensory sensitivities of neurons in the deep cerebellar nuclei were dynamically modulated on the basis of the difference between predictive and feedback signals consistent with the computation of sensory prediction error during motor learning. Prior single-unit recording studies have shown that these same neurons robustly encode vestibular sensory inputs during unexpected applied motion[24,41,42], but are not sensitive to the same vestibular sensory input when it is the result of self-generated motion[26]. We found that, in conditions that require motor learning, neuronal responses are correspondingly consistent with the trial-by-trial updating of a forward model, which minimizes the mismatch between expected and actual sensory input with the same temporal dynamics observed in the fine-tuning of motor commands required by the learning process. Thus, during motor learning, the responses of neurons in the deep cerebellar nuclei, which constitute a major output of the cerebellar cortex, suggest that the dynamic computation of a sensory prediction error signal underlies the brain's ability to both distinguish between expected and unexpected sensory inputs and learn new expected consequences of self-motion when unexpected sensory input becomes expected.

Neuronal computations that drive motor learning

Although it is generally agreed that the cerebellar cortex is required for initially driving motor learning and then ensuring that movements remain accurately calibrated over time (reviewed in refs. 14,43), its precise contribution remains controversial[10,11]. Nevertheless, the recent demonstration that cerebellar Purkinje cells encode the predicted consequence of movement rather than actual movement[12,44] provides strong support for the idea that the cerebellar cortex acts as a forward model. If motor learning is driven by the error signal computed by comparing this forward model's prediction of sensory feedback with the actual sensory feedback, then it follows that there should be evidence for such a computation. Notably, the computation of sensory prediction error theoretically requires that these two sensory-related signals be aligned in time as well as within the same neuronal location[4]. Accordingly, if these two representations are temporally offset in individual Purkinje cells, as recently suggested[13,19], then it follows that sensory prediction error is likely computed downstream of the Purkinje cells. This then raises the question of where and how does this computation occur?

We think our experimental findings provide new insight into this question by establishing that, during motor learning, neurons at the next stage of cerebellar processing (that is, in the deep cerebellar nuclei) robustly encode sensory reafference following the introduction of a sensory prediction error, such that they respond as if the stimuli were externally generated. Specifically, when the motor requirements changed, as was the case when we applied resistive torque to the head during voluntary movements (that is, learning) or removed it following learning (that is, extinction), there was initially a mismatch between the brain's prediction of the sensory consequences of the voluntary head motion and actual sensory feedback. Trial-by-trial analysis of rFN neuronal responses further revealed that the dynamic computation of sensory prediction error rapidly updated neuronal responses as the motor system learned to expect unexpected sensory input, suggesting successful temporal alignment between an internal estimate of the sensory consequences of self-generated head motion (that is, forward model) and its actual sensory feedback. Notably, neuronal responses were characterized by a decrease in sensitivity (that is, response gain), as the difference between expected and actual sensory input was minimized during both learning and extinction. Thus, although neuronal responses provide evidence for the dynamic computation of sensory prediction error, they do not explicitly encode the difference between expected and actual sensory input. Further studies of how rFN neurons integrate convergent input from cerebellar regions such as the anterior vermis[45] will be required to address this question.

Implications for the maintenance of accurate postural control

Our results have direct implications for behavior, as neurons in the fastigial deep cerebellar nucleus send descending projections to VN neurons that mediate vestibulo-spinal reflexes[46]. Given that these reflexes are essential for maintaining posture and balance, our ability to adapt their descending commands in the face of changes to either the motor apparatus or external environment is crucial. This is true for both continuous changes in the motor system (for example, changes in muscle fatigability, muscle fiber composition) and more abrupt changes in the external world. Indeed, our trial-by-trial analysis of learning-induced modulation of response sensitivity revealed the same temporal characteristics for neurons in the deep cerebellar and VN. These changes in neuronal activity occurred in a continuous, but rapid, manner with approximately the same time constant as the adaptive change in behavior, and, consistent with previous studies, the extinction of learning occurred faster than the initial learning itself (reviewed in ref. 32).

We posit that rapid updating observed at the level of single cerebellar output neurons is essential for ensuring stable perception and accurate motor control during our everyday activities. Both depend strongly on the integration of vestibular, proprioceptive and motor-related signals and are substantially disrupted in cerebellar patients[47]. The rFN receives descending projections from the anterior vermis of the cerebellum[20], and it in turn projects to vestibular neurons, reticular formation and spinal cord[20–23]. Following the introduction of a large sensory prediction error (for example, if we slip on ice) reflex pathways that mediate postural reflexes are robustly activated to maintain balance. In contrast, during volitional movement, the same pathways are markedly suppressed at the level of both the rFN and VN[26,34]. Hypothetically, this suppression is functionally advantageous, as an intact reflex would be counterproductive to the intended movement. Indeed, our results show that, as unexpected sensory input becomes expected, the mechanism underlying the suppression of sensory reafference is rapidly and accurately updated to re-enable this vital distinction between self-generated and applied stimulation.

METHODS

Methods and any associated references are available in the online version of the paper.

Note: Any Supplementary Information and Source Data files are available in the online version of the paper.

ACKNOWLEDGMENTS

We thank M. Chacron, M. Jamali, D. Mitchell, A. Dale and I. Mackrous for helpful discussions and critical reading of the manuscript, W. Kucharski for mechanical expertise and S. Nuara for animal care assistance. This study was supported by grants from the Canadian Institute of Health Research (MOP-42440), US National Institutes of Health (R01 DC002390) and from the Fonds Québécois de la Recherche sur la Nature et les Technologies to J.X.B.

AUTHOR CONTRIBUTIONS

J.X.B., J.C. and K.E.C. designed the study. J.X.B. and J.C. performed the experiments. J.X.B. and J.C. analyzed the data. K.E.C., J.X.B. and J.C. wrote the paper.

COMPETING FINANCIAL INTERESTS
The authors declare no competing financial interests.

Reprints and permissions information is available online at http://www.nature.com/reprints/index.html.

1. Bhushan, N. & Shadmehr, R. Computational nature of human adaptive control during learning of reaching movements in force fields. *Biol. Cybern.* **81**, 39–60 (1999).
2. Kawato, M. Internal models for motor control and trajectory planning. *Curr. Opin. Neurobiol.* **9**, 718–727 (1999).
3. Shadmehr, R., Smith, M.A. & Krakauer, J.W. Error correction, sensory prediction and adaptation in motor control. *Annu. Rev. Neurosci.* **33**, 89–108 (2010).
4. Wolpert, D.M. & Ghahramani, Z. Computational principles of movement neuroscience. *Nat. Neurosci.* **3** (suppl.) 1212–1217 (2000).
5. Wolpert, D.M. & Miall, R.C. Forward models for physiological motor control. *Neural Netw.* **9**, 1265–1279 (1996).
6. Berniker, M. & Kording, K. Estimating the sources of motor errors for adaptation and generalization. *Nat. Neurosci.* **11**, 1454–1461 (2008).
7. Todorov, E. & Jordan, M.I. Optimal feedback control as a theory of motor coordination. *Nat. Neurosci.* **5**, 1226–1235 (2002).
8. Mazzoni, P. & Krakauer, J.W. An implicit plan overrides an explicit strategy during visuomotor adaptation. *J. Neurosci.* **26**, 3642–3645 (2006).
9. Wong, A.L. & Shelhamer, M. Sensorimotor adaptation error signals are derived from realistic predictions of movement outcomes. *J. Neurophysiol.* **105**, 1130–1140 (2011).
10. Ebner, T.J., Hewitt, A.L. & Popa, L.S. What features of limb movements are encoded in the discharge of cerebellar neurons? *Cerebellum* **10**, 683–693 (2011).
11. Medina, J.F. The multiple roles of Purkinje cells in sensori-motor calibration: to predict, teach and command. *Curr. Opin. Neurobiol.* **21**, 616–622 (2011).
12. Pasalar, S., Roitman, A.V., Durfee, W.K. & Ebner, T.J. Force field effects on cerebellar Purkinje cell discharge with implications for internal models. *Nat. Neurosci.* **9**, 1404–1411 (2006).
13. Popa, L.S., Hewitt, A.L. & Ebner, T.J. Predictive and feedback performance errors are signaled in the simple spike discharge of individual Purkinje cells. *J. Neurosci.* **32**, 15345–15358 (2012).
14. Krakauer, J.W. & Mazzoni, P. Human sensorimotor learning: adaptation, skill and beyond. *Curr. Opin. Neurobiol.* **21**, 636–644 (2011).
15. Wolpert, D.M., Goodbody, S.J. & Husain, M. Maintaining internal representations: the role of the human superior parietal lobe. *Nat. Neurosci.* **1**, 529–533 (1998).
16. Bastian, A.J. Learning to predict the future: the cerebellum adapts feedforward movement control. *Curr. Opin. Neurobiol.* **16**, 645–649 (2006).
17. Taylor, J.A., Klemfuss, N.M. & Ivry, R.B. An explicit strategy prevails when the cerebellum fails to compute movement errors. *Cerebellum* **9**, 580–586 (2010).
18. Tseng, Y.W., Diedrichsen, J., Krakauer, J.W., Shadmehr, R. & Bastian, A.J. Sensory prediction errors drive cerebellum-dependent adaptation of reaching. *J. Neurophysiol.* **98**, 54–62 (2007).
19. Popa, L.S., Hewitt, A.L. & Ebner, T.J. Purkinje cell simple spike discharge encodes error signals consistent with a forward internal model. *Cerebellum* **12**, 331–333 (2013).
20. Batton, R.R. III, Jayaraman, A., Ruggiero, D. & Carpenter, M.B. Fastigial efferent projections in the monkey: an autoradiographic study. *J. Comp. Neurol.* **174**, 281–305 (1977).
21. Carleton, S.C. & Carpenter, M.B. Afferent and efferent connections of the medial, inferior and lateral vestibular nuclei in the cat and monkey. *Brain Res.* **278**, 29–51 (1983).
22. Homma, Y., Nonaka, S., Matsuyama, K. & Mori, S. Fastigiofugal projection to the brainstem nuclei in the cat: an anterograde PHA-L tracing study. *Neurosci. Res.* **23**, 89–102 (1995).
23. Shimazu, H. & Smith, C.M. Cerebellar and labyrinthine influences on single vestibular neurons identified by natural stimuli. *J. Neurophysiol.* **34**, 493–508 (1971).
24. Brooks, J.X. & Cullen, K.E. Multimodal integration in rostral fastigial nucleus provides an estimate of body movement. *J. Neurosci.* **29**, 10499–10511 (2009).
25. Roy, J.E. & Cullen, K.E. Selective processing of vestibular reafference during self-generated head motion. *J. Neurosci.* **21**, 2131–2142 (2001).
26. Brooks, J.X. & Cullen, K.E. The primate cerebellum selectively encodes unexpected self-motion. *Curr. Biol.* **23**, 947–955 (2013).
27. Kluzik, J., Diedrichsen, J., Shadmehr, R. & Bastian, A.J. Reach adaptation: what determines whether we learn an internal model of the tool or adapt the model of our arm? *J. Neurophysiol.* **100**, 1455–1464 (2008).
28. Lackner, J.R. & DiZio, P. Adaptation to Coriolis force perturbation of movement trajectory; role of proprioceptive and cutaneous somatosensory feedback. *Adv. Exp. Med. Biol.* **508**, 69–78 (2002).
29. Scheidt, R.A., Conditt, M.A., Secco, E.L. & Mussa-Ivaldi, F.A. Interaction of visual and proprioceptive feedback during adaptation of human reaching movements. *J. Neurophysiol.* **93**, 3200–3213 (2005).
30. Zago, M. *et al.* Fast adaptation of the internal model of gravity for manual interceptions: evidence for event-dependent learning. *J. Neurophysiol.* **93**, 1055–1068 (2005).
31. Lackner, J.R. & DiZio, P.A. Adaptation to rotating artificial gravity environments. *J. Vestib. Res.* **13**, 321–330 (2003).
32. Shadmehr, R. & Mussa-Ivaldi, F.A. Adaptive representation of dynamics during learning of a motor task. *J. Neurosci.* **14**, 3208–3224 (1994).
33. Shadmehr, R. Control of movements and temporal discounting of reward. *Curr. Opin. Neurobiol.* **20**, 726–730 (2010).
34. Roy, J.E. & Cullen, K.E. Dissociating self-generated from passively applied head motion: neural mechanisms in the vestibular nuclei. *J. Neurosci.* **24**, 2102–2111 (2004).
35. Rabe, K. *et al.* Adaptation to visuomotor rotation and force field perturbation is correlated to different brain areas in patients with cerebellar degeneration. *J. Neurophysiol.* **101**, 1961–1971 (2009).
36. Smith, M.A. & Shadmehr, R. Intact ability to learn internal models of arm dynamics in Huntington's disease but not cerebellar degeneration. *J. Neurophysiol.* **93**, 2809–2821 (2005).
37. Werner, S., Bock, O. & Timmann, D. The effect of cerebellar cortical degeneration on adaptive plasticity and movement control. *Exp. Brain Res.* **193**, 189–196 (2009).
38. Barash, S. *et al.* Saccadic dysmetria and adaptation after lesions of the cerebellar cortex. *J. Neurosci.* **19**, 10931–10939 (1999).
39. Rambold, H., Churchland, A., Selig, Y., Jasmin, L. & Lisberger, S.G. Partial ablations of the flocculus and ventral paraflocculus in monkeys cause linked deficits in smooth pursuit eye movements and adaptive modification of the VOR. *J. Neurophysiol.* **87**, 912–924 (2002).
40. Izawa, J. & Shadmehr, R. Learning from sensory and reward prediction errors during motor adaptation. *PLOS Comput. Biol.* **7**, e1002012 (2011).
41. Gardner, E.P. & Fuchs, A.F. Single-unit responses to natural vestibular stimuli and eye movements in deep cerebellar nuclei of the alert rhesus monkey. *J. Neurophysiol.* **38**, 627–649 (1975).
42. Shaikh, A.G., Ghasia, F.F., Dickman, J.D. & Angelaki, D.E. Properties of cerebellar fastigial neurons during translation, rotation, and eye movements. *J. Neurophysiol.* **93**, 853–863 (2005).
43. Lisberger, S.G. Internal models of eye movement in the floccular complex of the monkey cerebellum. *Neuroscience* **162**, 763–776 (2009).
44. Hewitt, A.L., Popa, L.S., Pasalar, S., Hendrix, C.M. & Ebner, T.J. Representation of limb kinematics in Purkinje cell simple spike discharge is conserved across multiple tasks. *J. Neurophysiol.* **106**, 2232–2247 (2011).
45. Barresi, M., Bruschini, L., Li Volsi, G. & Manzoni, D. Effects of leg-to-body position on the responses of rat cerebellar and vestibular nuclear neurons to labyrinthine stimulation. *Cerebellum* **11**, 212–222 (2012).
46. Wilson, V.J., Yamagata, Y., Yates, B.J., Schor, R.H. & Nonaka, S. Response of vestibular neurons to head rotations in vertical planes. III. Response of vestibulocollic neurons to vestibular and neck stimulation. *J. Neurophysiol.* **64**, 1695–1703 (1990).
47. Kammermeier, S., Kleine, J. & Buttner, U. Vestibular-neck interaction in cerebellar patients. *Ann. NY Acad. Sci.* **1164**, 394–399 (2009).

ONLINE METHODS

Two adult male rhesus monkeys (*Macaca mulatta*) were prepared for chronic extracellular recording using aseptic surgical techniques. Monkeys were housed in pairs and kept on a 12-h dark/light cycle. All experimental protocols were approved by the McGill University Animal Care Committee and were in compliance with the guidelines of the Canadian Council on Animal Care.

Surgical procedures. Surgical techniques were similar to those previously described[24]. Briefly, under aseptic conditions and surgical levels of isoflurane an 18-mm diameter eye coil (three loops of Teflon-coated stainless steel wire) was attached to the sclera beneath the conjunctiva of one eye. In addition, a dental acrylic implant was fastened to the animal's skull using stainless steel screws. The implant held in place a stainless steel post used to restrain the animal's head, and a stainless steel recording chamber positioned to access the rFN and VN (posterior and lateral angles of 28° and 30°, respectively). Animals were given 2 weeks to recover from the surgery before any experiments were performed.

Data acquisition. During the experiments, conducted during the light period of the light/dark cycle, monkeys sat comfortably in a primate chair located on a vestibular turntable, and the animal's head was centered in a stationary 1-m^3 magnetic field coil system (CNC Engineering). Extracellular single-unit activity was recorded using enamel-insulated tungsten microelectrodes (7–10-MΩ impedance, Frederick-Haer). The location of the rFN and VN was determined relative to the abducens nucleus, which was identified based on its stereotypical neuronal responses during eye movements. Turntable velocity was measured using an angular velocity sensor (Watson Industries). Gaze and head positions were measured using the magnetic search coil technique as previously described[24,25]. During experiments, unit activity, horizontal gaze, head and target positions, and table velocity were recorded on DAT tape for later playback. Action potentials were discriminated during playback using a windowing circuit (BAK) that was manually set to generate a pulse coincident with the rising phase of each action potential. Gaze, head and target position, and table velocity signals were low-pass filtered at 250 Hz (8 pole anti-aliasing Bessel filter) and sampled at 1,000 Hz.

Behavioral procedures. *Head-restrained procedures.* Monkeys were trained to follow a target light (HeNe laser) that was projected, via a system of two galvanometer-controlled mirrors, onto a cylindrical screen located 60 cm away from the monkey's head. Target, turntable motion, torque motor and data displays were controlled on-line by a UNIX-based real-time data-acquisition system (REX, Laboratory of Sensorimotor Research, US National Institutes of Health). Consistent with previous studies of rFN and VN, all neurons were sensitive to passive vestibular stimulation but not to eye movements[41]. Accordingly, to verify that neurons were unresponsive to eye movements, neuronal activity was recorded during saccades and periods of fixation when head-restrained monkeys followed a target that stepped between horizontal positions over a range of ±30°. Neuronal responses were also recorded during smooth pursuit eye movements made to track sinusoidal target motion (0.5 Hz, 40° per s peak velocity).

Neuronal sensitivities to vestibular stimulation were verified by passively rotating monkeys about an earth vertical axis in the dark (whole-body rotation) and also during a paradigm in which they suppressed the vestibulo-ocular reflex (VOR) by fixating a laser target that moved with the vestibular turntable (termed VOR cancellation (VORc)). The responses of neurons in both the rFN and VN were comparable during VOR and VORc ($P > 0.05$), consistent with these neurons' insensitivity to eye motion. We characterized responses to whole-body rotation using two types of stimulation: a 1-Hz sine wave with peak velocity of ± 40 ° per s and a typical head velocity trajectory generated during active gaze shifts in the head-unrestrained condition, termed 'active-like motion' profile. The latter stimulus was used to facilitate comparison of neuronal responses during passive and active (see below) head rotations.

Head-unrestrained procedures. After a neuron was fully characterized in the head-restrained condition, the monkey's head was slowly and carefully released to maintain isolation. Once released, the monkey was able to only rotate its head in the yaw axis (that is, earth-vertical rotation) with no pitch or roll rotation or translations. The response of the same neuron was then recorded during the voluntary head movements made while orienting to a laser target projected on a screen in front of the monkey for a juice reward. The target alternated from between a position 25 degrees to the right and one 25 degrees to the left of midline. Monkeys were required to remain on target at the end of the head movement for 500 ms to receive a reward.

Next, using a torque motor (Kollmorgen), we applied a resistive torque to the head while the monkeys made active head movements (**Fig. 1b**). This torque was proportional to head velocity and was calibrated such that initially head velocity was reduced by approximately half that observed during control active head movements. One trial consisted of a leftward and then rightward head rotation. For simplicity, we show responses in the neuron's preferred direction. The resistive torque was then kept constant while the monkey learned to adjust his head movements to acquire the target (**Fig. 1c**; learning phase). During the last third of the learning phase, we introduced random trials, during which no resistive torque was applied (**Fig. 1c**; catch trials). Finally we stopped applying the resistive torque for an extended period of time while the monkey continued to orient to the targets and once again needed to change his head movements in order to acquire the target (**Fig. 1c**; extinction phase).

Analysis of neuronal discharges. Data were imported into the Matlab (MathWorks) programming environment for analysis. Recorded gaze and head position signals were digitally filtered with zero-phase at 60 Hz using a 51st-order finite-impulse-response (FIR) filter with a Hamming window. Eye position was calculated from the difference between gaze and head position signals. Gaze, eye and head position signals were digitally differentiated to produce velocity signals. Neural firing rate was represented using a spike density function in which a Gaussian was convolved with the spike train s.d. of 5 ms as previously described[24,25].

To determine whether a unit could be classified as a VO neuron, we first verified that it was unresponsive to eye position and/or velocity by analyzing periods of steady fixation and saccade-free smooth pursuit using a multiple regression analysis[24,25]. In addition, spike trains were assessed to confirm that neurons neither paused nor burst during saccades. Prior characterizations of these same neurons have shown that their responses to head motion are well described by a second order head-velocity based equation[24,25]. Accordingly, a least-squared regression analysis was then used to describe each unit's response to head motion stimulation during passive and active head rotations

$$\widehat{fr}(t) = b + S_v\dot{H}(t) + S_a\ddot{H} \quad (1)$$

where $\widehat{fr}$ is the estimated firing rate, S_v and S_a are coefficients representing sensitivities to head velocity and acceleration, b is a bias term, and $\dot{H}$ and $\ddot{H}$ are head velocity and head acceleration, respectively. Note that this equation could be used during passive or active motion as well as during the learning and extinction protocols. Only data for which the firing rate was greater than 20 spikes per s were included in regression analyses.

To quantify the ability of the linear regression analysis to model neuronal discharges, we determined variance-accounted-for (VAF) provided by each regression equation. The VAF was computed as

$$VAF = 1 - [var(\widehat{fr} - fr)/var(fr)] \quad (2)$$

where $\widehat{fr}$ represents the modeled firing rate (that is, regression equation estimate) and fr represents the actual firing rate.

The regression analyses were first applied to data collected in the control passive and active motion conditions to obtain estimates of neuronal sensitivity in each condition before learning. The regression analyses were then applied to data collected during the learning phase to estimate average sensitivities for the first five, middle five (26–30) and last five (46–50) head movements to calculate estimates of the average peak head velocity and neuronal sensitivity for the early, middle and late phases of learning (the average peak head velocity was normalized relative to the passive peak head velocity). Finally, to quantify the detailed time course of the changes in behavior and neuronal sensitivity, we applied the regression analysis to individual head movements as well as obtained the peak velocity for each head movement.

To facilitate comparison across neurons, we normalized both peak head velocity and neuronal sensitivity. Peak head velocity during the learning paradigm was normalized using

$$\dot{H}_E = (H_a - H_n)/(H_a - H_1) \quad (3)$$

doi:10.1038/nn.4077

where $\dot{H}_E$ is the normalized error in peak velocity, H_a is the head velocity during the control active phase, H_n is the head velocity on a given trial and H_1 is the head velocity on the first trial. This equation results in values near 0 when peak head velocity is comparable to that produced for control active movements before learning and of 1 when the resistive torque is initially applied and head velocity is most drastically attenuated. Similarly, peak head velocity (H_{pk}) during learning extinction was normalized using

$$H_{pk} = (H_n - H_a)/(H_1 - H_a) \tag{4}$$

and neuronal sensitivities during learning and extinction were normalized using

$$N = x/P \tag{5}$$

where N is the normalized sensitivity, x is the sensitivity on a given trial and P is the sensitivity during passive head motion. Equation (5) results in values near 1 when the sensitivity is the same as during passive head movements. We then fit this trial-by-trial data with an exponential curve and calculated a time constant for changes in both peak head velocity and neuronal sensitivity.

Statistics. No statistical methods were used to predetermine sample sizes, but our sample sizes are similar to those generally employed in the field[26]. Before statistical analysis, normality of distribution was evaluated using Kolmogorov-Smirnov test. Statistical significance ($P < 0.05$) was determined using non-parametric analysis with either two-tailed Wilcoxon signed-rank or rank-sum test. Data are expressed as mean ± s.e.m.

A **Supplementary Methods Checklist** is available.